

Molecular docking studies on the phytoconstituents as therapeutic leads against SARS-CoV-2

Abhishek Tiwari^{1), *} (ORCID ID: 0000-0003-1221-4754), Varsha Tiwari¹⁾ (0000-0002-2293-8943), Navneet Verma¹⁾ (0000-0002-3803-8456), Anita Singh²⁾ (0000-0003-2149-1155), Manish Kumar³⁾ (0000-0003-2042-1243), Vipin Saini³⁾ (0000-0003-2881-042X), Biswa Mohan Sahoo⁴⁾ (0000-0001-8822-0427), Deepak Kaushik⁵⁾ (0000-0002-3286-196X), Ravinder Verma⁶⁾ (0000-0003-3397-703X), Suresh Sagadevan^{7), *} (0000-0003-0393-7344)

DOI: <https://doi.org/10.14314/polimery.2022.7.8>

Abstract: Because of the present pandemic researchers are seeking for phytocandidates that can inhibit or stop SARS-CoV-2. The main protease (M^{Pro}) of SARS-CoV-2 and spike glycoprotein (S) are both suppressed by bioactive compounds found in plants that work by docking them together. The M^{Pro} proteins 6LU7 (complex with an inhibitor N3) and 5C3N (space group C2221) were employed in docking research. PyRx and AutoDock Vina software were used as docking engine. 22 identified phytoconstituents were selected from IMPPAT, a manually curated database, on the basis of their antiviral effects. Docking studies showed that phytoconstituents β -amyryn (-8.4 kcal/mol), withaferin A (-8.3 kcal/mol), oleanolic acid (-7.8 kcal/mol), and patentiflorin A (-8.1 kcal/mol) had the best results against 5C3N M^{Pro} protein whereas kuwanon L (-7.1 kcal/mol), β -amyryn (-6.9 kcal/mol), oleanolic acid (-6.8 kcal/mol), cucurbitacin D (-6.5 kcal/mol), and quercetin (-6.5 kcal/mol) against 6LU7 M^{Pro} protein. All the compounds were examined for their ADMET characteristics using SwissDock. Present research reports that the phytoconstituents along with docking score will be helpful for future drug development against Covid-19.

Keywords: Covid-19, spike glycoprotein, AutoDock Vina, M^{Pro}, docking, artemisinin, withaferin A.

Molekularne badania dokujące nad zastosowaniem fitoskładników w terapii przeciw SARS-CoV-2

Streszczenie: W związku z pandemią prowadzone są badania mające na celu znalezienie fitosubstancji, które mogą hamować lub zatrzymać rozwój SARS-CoV-2. Działanie głównych białek proteazy (M^{Pro}) SARS-CoV-2 i glikoproteiny kolca (S) jest osłabiane przez związki bioaktywne występujące w roślinach poprzez proces dokowania. Do badań dokujących użyto białka M^{Pro} 6LU7 (kompleks z inhibitorem N3) i 5C3N (grupa przestrzenna C2221). Jako silnik dokujący zastosowano PyRx i AutoDock Vina. Zidentyfikowano 22 fitoskładniki wybrane z bazy danych IMPPAT, z uwzględnieniem ich działania przeciwwirusowego. Najbardziej skuteczne w przypadku białka M^{Pro} 5C3N okazały się fitoskładniki β -amyryna (-8,4 kcal/mol), witaferyna A (-8,3 kcal/mol), kwas oleanolowy (-7,8 kcal/mol) i patentifloryna A (-8,1 kcal/mol), a w przypadku białka M^{Pro} 6LU7 kuwanon L (-7,1 kcal/mol), β -amyryna (-6,9 kcal/mol), kwas oleanolowy (-6,8 kcal/mol), kukurbitacyna D (-6,5 kcal/mol) i kwercetyna (-6,5 kcal/mol). Wszystkie substancje zbadano pod kątem ich właściwości ADMET przy użyciu SwissDock. Wykazano, że fitoskładniki mogą być pomocne w pracach nad lekami przeciwko Covid-19.

Słowa kluczowe: Covid-19, glikoproteina kolca, AutoDock Vina, M^{Pro}, dokowanie, artemizynina, witaferyna A.

¹⁾ Pharmacy Academy, IFTM University, Moradabad-244102, Uttar Pradesh, India.

²⁾ Department of Pharmaceutical Sciences, Kumaun University, Bhimtal Campus, Nainital, Uttarakhand-263136 India.

³⁾ MM College of Pharmacy, Maharishi Markandeshwar (Deemed to be University), Mullana, Ambala-133207, Haryana India.

⁴⁾ Roland Institute of Pharmaceutical Sciences, Berhampur, Odisha-760010, India.

⁵⁾ Department of Pharmaceutical Sciences, M.D. University, Rohtak (124001), Haryana, India.

⁶⁾ Department of Pharmacy, G.D. Goenka University, Gurugram-122103, Haryana, India.

⁷⁾ Nanotechnology and Catalysis Research Centre, University of Malaya, Kuala Lumpur, Malaysia- 50603.

^{*} Authors for correspondence: drabhishekdv@gmail.com; drsureshnano@gmail.com

The novel coronavirus disease 2019 (Covid-19) outbreak, which was first detected in December 2019, has become a worldwide pandemic. Coronaviruses are positive-stranded RNA viruses with spike glycoproteins (S proteins) that resemble crowns under the electron microscope [1]. The ortho-coronavirinae subfamily is divided into 4 major genera namely alpha (α CoV), beta (β CoV),

delta (δ CoV), and gamma (γ CoV) within the *Coronaviridae* family [2]. According to the genomic study, bats and rodents are the outsource of α and β CoVs, respectively, whilst avian species are the source of δ and γ CoVs [3–5]. SARS-CoV-2 is enveloped by a single-stranded RNA. It is 29881 bp long (GenBank no. MN908947) and encodes 9 860 amino acids, and it was discovered using a metagenomic

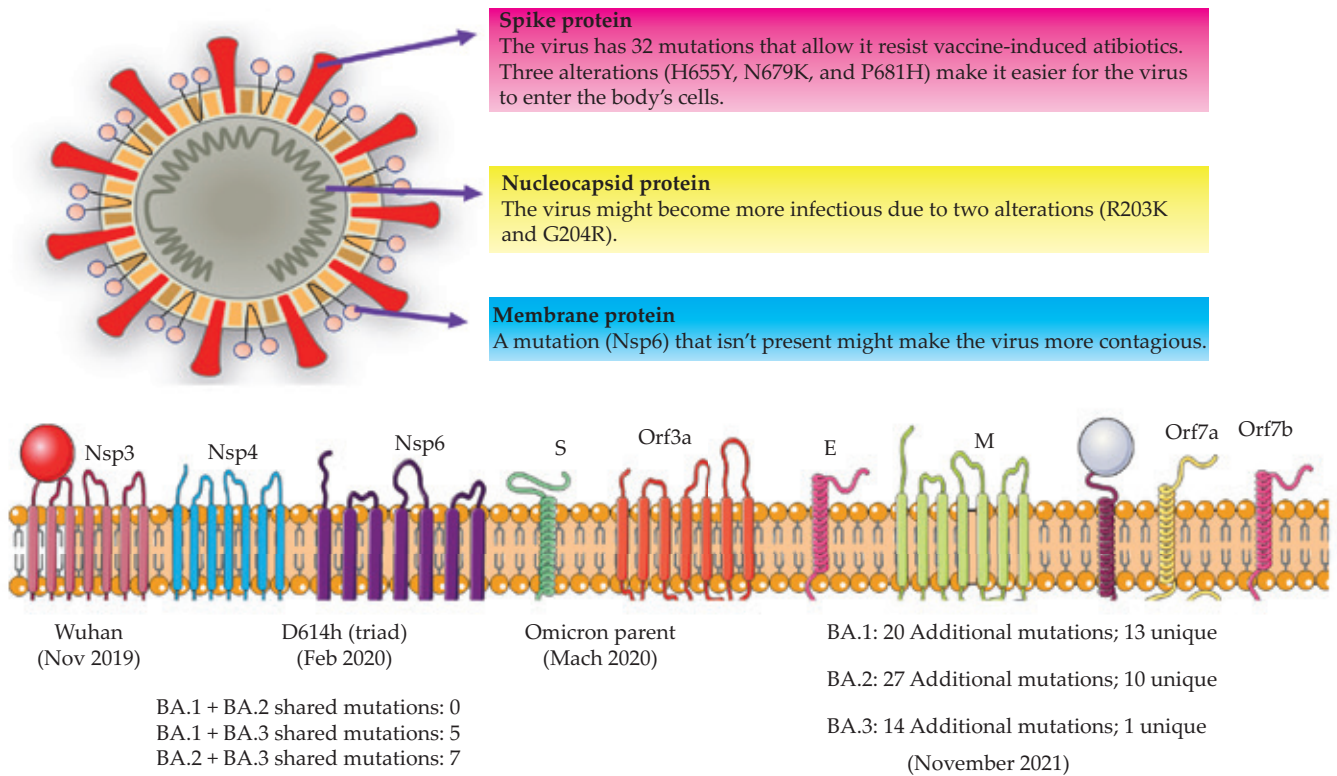


Fig. 1. SARS-CoV-2 structure and membrane proteins domains

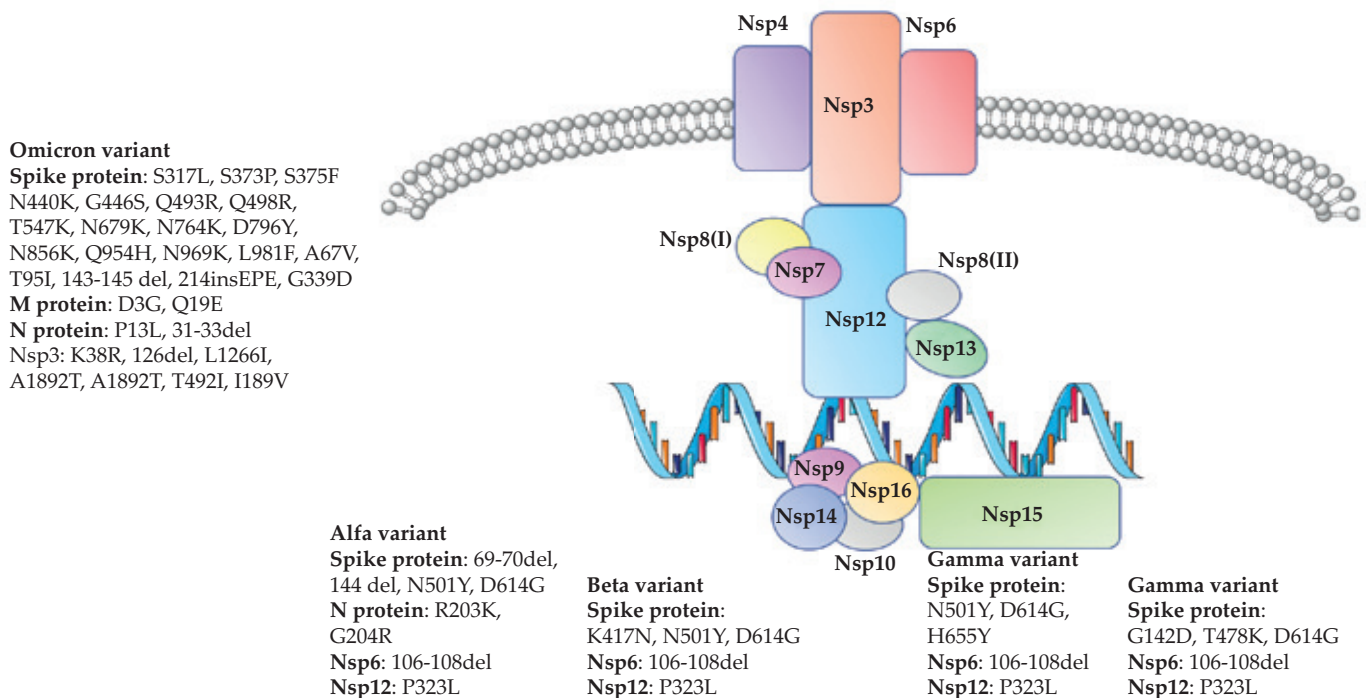


Fig. 2. Comparative visualization of various strains and mutations of SARS-CoV-2

Table 1. Omicron types of mutation: place and effect

Variant	Mutation	Position of mutations	Effect	References
Omicron B.1.1.529	36 amino acid-altering mutations, out of which 23 were observed in other variants as well	6 deletions at 69, 70, 143, 144, 145 and 211, of which 211 is unique	Deletions in immune evasion	[11]
	Other mutations at N-terminal including A67V observed in Eta (Nigeria) and T95I in Iota variant (New York) and G142D (Delta variant)	Insertion at 214 place exists, which includes 3 amino acids to genome	Boost ACE2 binding affinity	[11]
	Receptor-binding area possesses 15 amino acid substitutions out of which 11 were observed in other variants	Mutations at receptor-binding area E484A, N501Y, S477N, and K417N were observed	Plays significant role in boosting the efficiency of furin cleavage resulting in enhancement of the transmissibility	[11]
	Among the most concerning receptor-binding domain the other ones were previously observed in major variants of concern like alpha and delta	Includes K417N, N440K, S477N, E484A, G496S, Q498R, N501Y, and others	These mutations may contribute to augment the infectivity through promoting S protein fusion	[11]
	Furin cleavage mutations including T547K, H655Y, N679K, and P681H	Mutations at S2 subunit (N764K, D796Y, N856K, Q954H, N969K, and L981F)		

Table 2. Variants of concern and variants of interest as per WHO

Variant	Pango lineage	Auxillary amino acid change	Announcement date	References
Variant of concern				
Alpha	B.1.1.7	+S:484K, +S:452R	18/12/2020	[11]
Beta	B.1.351	+S:L18F	18/12/2020	[11]
Gamma	P.1	+S:681H	11/01/2021	[11]
Delta	B.1.617.2	+S:417N, +S:484K	11/05/2021	[11]
Omicron	B.1.1.529	+S:R346K	26/11/2021	
Variant of interest				
Lambda	C.37	–	14/06/2021	[11]
Mu	B.1.621	–	30/08/2021	[11]

next-generation sequencing technique [6]. Two types of proteins are produced by gene fragmentation: structural and non-structural proteins. The S, E, M, and N genes encode structural proteins, whereas the Orf area encodes non-structural 3-chymotrypsin-like protease, papain-like protease, and RNA-dependent RNA polymerase. The S glycoproteins on the surface of SARS-CoV-2 interact with the ACE2 host cell receptor, making it easier for the virus to enter the cell (Figure 1). On the host cell membrane, the TM protease Serine 2 aids the S protein in entering and activating the cell [7–10]. Following the publishing of the SARS-CoV-2 genome sequence, there has been a substantial rise in research into the molecular mechanism of SARS-CoV-2 infection. Figure 2 and Table 1 reveal different types of mutation of SARS-CoV-2. Table 2 shows “variants of concern” and “variants of interest” for future drug development as specified by WHO [11–14]. Over two years after the start of the SARS-CoV-2 epidemic, which has killed

over 5 million people, the globe is still on high Covid-19 alert. In collaboration with national authorities, public health organizations, and scientists, the WHO has been intensively monitoring and analyzing the development of SARS-CoV-2 since January 2020 [11]. As a result, there is an urgent need for study in this area in order to discover a solution of this massive problem, because changes in the SARS-CoV-2 virus will continue. The current research is an honest attempt to investigate our natural phytocandidates for fighting SARS-CoV-2 and its mutations.

ROLE OF THE SARS-COV-2 MAIN PROTEASE

Typically, β CoVs generate pp1a (450–500 kDa) and pp1ab (300–400 kDa) by translating the genomic RNA (750–800 kDa) [15, 16]. Proteinases break down polypeptides like these into the structural and non-structural proteins the virus needs to replicate and assemble. This pro-

Table 3. Selected phytoconstituents and their therapeutic uses

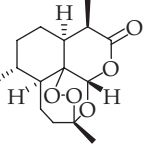
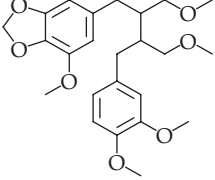
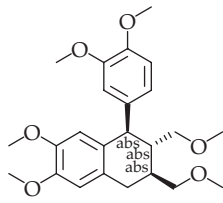
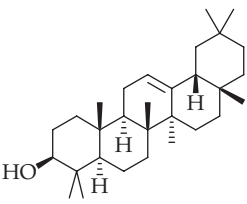
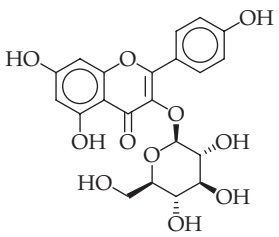
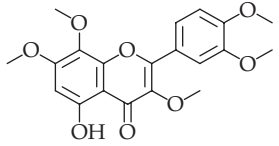
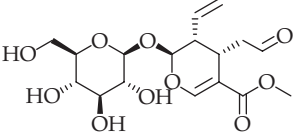
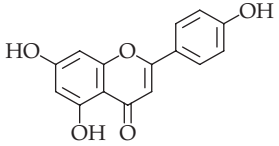
Phytoconstituent	ID	Structure	Reported therapeutic uses	Reference
Artemisinin	IMPHY007168		Antimalarial	[18]
Niranthin	IMPHY002597		Leishmania donovani topoisomerase IB	[19]
Phyltetralin	IMPHY000162		Immunomodulatory effects	[20]
β -Amyrin	IMPHY012223		Anti-inflammatory and antinociceptive, antioxidant, antipruritic, gastroprotective and hepatoprotective effects	[21]
Astragalin	IMPHY014963		Anti-inflammatory, anti-allergic	[22]
5-Hydroxy-3,7,8,3',4'-pentamethoxyflavone	IMPHY002586		Anti-allergic, anti-inflammatory	[23]
Secologanin	IMPHY001714		Analgesic, anti-inflammatory, antiarthritic, anti-allergenic, antibacterial and antiviral	[24]
Apigenin	IMPHY004661		Anti-inflammatory, anticancer, antioxidative, and antiviral	[25]

Table 3. cont.

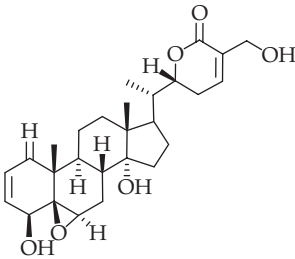
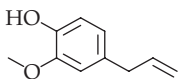
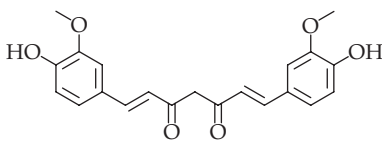
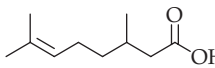
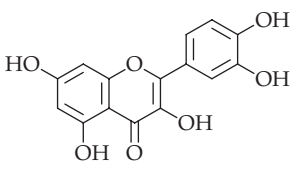
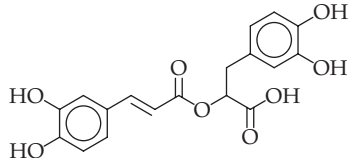
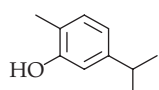
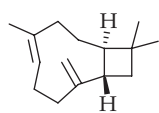
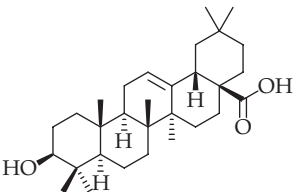
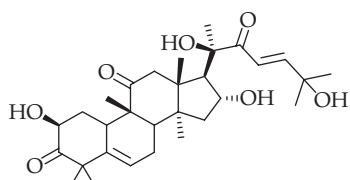
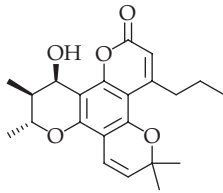
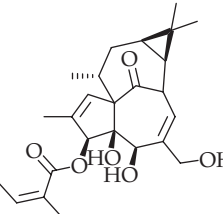
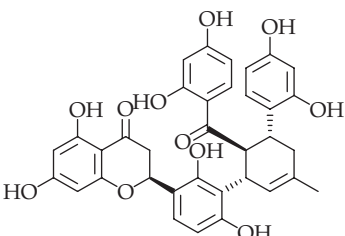
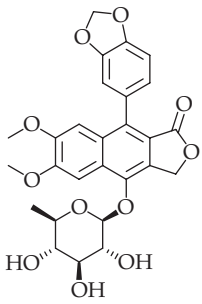
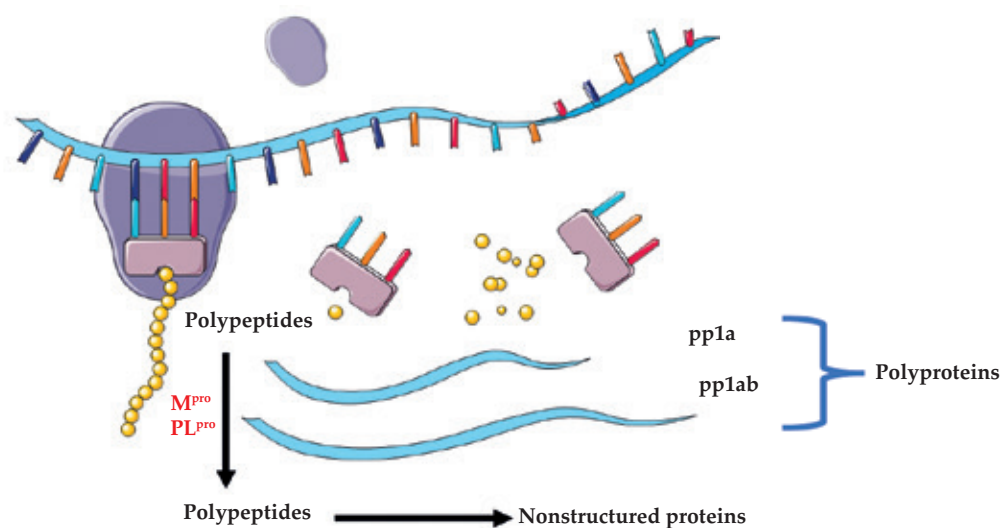
Phytoconstituent	ID	Structure	Reported therapeutic uses	Reference
Withaferin A	IMPHY004118		Anticancer potential, anti-angiogenesis	[26]
Eugenol	IMPHY003536		Analgesic and antiseptic, flavoring agent	[27]
Curcumin	IMPHY007574		Anti-inflammatory, hypoglycemic, antioxidant, wound-healing, antimicrobial	[28]
Citronellic acid	IMPHY001084		Cytotoxic, excellent modulatory effect	[29]
Quercetin	IMPHY004619		Antioxidant and anti-inflammatory, reduces swelling, kills cancer cells, controls blood sugar, and helps preventing heart diseases	[30]
Rosmarinic acid	IMPHY004597		Antimicrobial, immunomodulatory, antidiabetic, anti-allergic, anti-inflammatory, hepato- and renalprotectant agent, beneficial effects during skin afflictions	[31]
Carvacrol	IMPHY001246		Antibacterial, anticancer, antimutagenic, antigenotoxic, analgesic, antispasmodic, anti-inflammatory, angiogenic, antiparasitic, antiplatelet, AChE inhibitory, insecticidal, antihepatotoxic, hepatoprotective	[32]
β -Caryophyllene	IMPHY014831		Cardioprotective, hepatoprotective, gastroprotective, neuroprotective, nephroprotective, antioxidant, anti-inflammatory, antimicrobial, immunomodulator	[33]
Oleanolic acid	IMPHY014831		Ulcerative colitis, multiple sclerosis, metabolic disorders, diabetes, hepatitis, and different cancers	[34]
Cucurbitacin D	IMPHY011825		Anticancer, induces apoptosis	[35]

Table 3. cont.

Phytoconstituent	ID	Structure	Reported therapeutic uses	Reference
Calanolide B	IMPHY004599		Anti-HIV activity, anticancer, antimicrobial, antiparasitic	[36]
Ingenol	IMPHY004935		Treatment of actinic keratosis	[37]
Kuwanon L	IMPHY000943		Anti-inflammatory, antimicrobial, antimelanogenic, renoprotective, hepatoprotective	[38]
Patentiflorin A	IMPHY005292		Anti-HIV potential.	[39]



The polyproteins are broken into 16 NSP1-16. A-1 ribosomal frameshift is required to produce the longer (PP1ab) or shorter (PP1a). It contains proteins that other coronaviruses have, such as a papain-like (Nsp3), 3C-like (Nsp5), RdRp (RNA-dependent RNA polymerase, HEL (helix-like), endoRNase (Nsp15), 2'-O-Ribose-Methyltransferase (Nsp16), and other nonstructural proteins. **They control viral transcription, replication, proteolytic processing, suppressing host immune responses and gene expressions.**

Fig. 3. Role of M^{pro} in SARS-CoV-2

Table 4. Physicochemical properties of selected phytocandidates

Molecule name	Formula	Molecular weight g/mol	No. of heavy atoms	No. of arom. heavy atoms	Fraction Csp3	No. of rotatable bonds	No. of H-bond acceptors	No. of H-bond donors	MR	TPSA, Å ²
Artemisinin	C ₁₅ H ₂₂ O ₅	282.33	20	0	0.93	0	5	0	70.38	53.99
Niranthin	C ₂₄ H ₃₂ O ₇	432.51	31	12	0.50	12	7	0	117.25	64.61
Phyltetralin	C ₂₄ H ₃₂ O ₆	416.51	30	12	0.50	9	6	0	115.73	55.38
Astragalin	C ₂₁ H ₂₀ O ₁₁	448.38	32	16	0.29	4	11	7	108.13	190.28
5-Hydroxy-3,7,8,3',4'-pentamethoxyflavone	C ₂₀ H ₂₀ O ₈	388.37	28	16	0.25	6	8	1	102.40	96.59
Secologanin	C ₁₇ H ₂₄ O ₁₀	388.37	27	0	0.65	8	10	4	88.04	151.98
Apigenin	C ₁₅ H ₁₀ O ₅	270.24	20	16	0.00	1	5	3	73.99	90.90
Withaferin A	C ₂₈ H ₃₈ O ₆	470.60	34	0	0.79	3	6	2	127.49	96.36
Eugenol	C ₁₀ H ₁₂ O ₂	164.20	12	6	0.20	3	2	1	49.06	29.46
Curcumin	C ₂₁ H ₂₀ O ₆	368.38	27	12	0.14	8	6	2	102.80	93.06
Citronellic acid	C ₁₀ H ₁₈ O ₂	170.25	12	0	0.70	5	2	1	51.48	37.30
Quercetin	C ₁₅ H ₁₀ O ₇	302.24	22	16	0.00	1	7	5	78.03	131.36
Rosmarinic acid	C ₁₈ H ₁₆ O ₈	360.31	26	12	0.11	7	8	5	91.40	144.52
Carvacrol	C ₁₀ H ₁₄ O	150.22	11	6	0.40	1	1	1	48.01	20.23
Ingenol	C ₂₀ H ₂₈ O ₅	348.43	25	0	0.75	1	5	4	93.22	97.99
Calanolide B	C ₂₂ H ₂₆ O ₅	370.44	27	10	0.50	2	5	1	106.11	68.90
β-Amyrin	C ₃₀ H ₅₀ O	426.72	31	0	0.93	0	1	1	134.88	20.23
β-Caryophyllene	C ₁₅ H ₂₄	204.35	15	0	0.73	0	0	0	68.78	0.00
Oleanolic acid	C ₃₀ H ₄₈ O ₃	456.70	33	0	0.90	1	3	2	136.65	57.53
Cucurbitacin D	C ₃₀ H ₄₄ O ₇	516.67	37	0	0.77	4	7	4	141.20	132.13
Kuwanon L	C ₃₅ H ₃₀ O ₁₁	626.61	46	24	0.20	5	11	8	167.11	205.21
Patentiflorin A	C ₂₇ H ₂₆ O ₁₁	526.49	38	16	0.37	5	11	3	130.74	142.37

Csp3 – ratio of sp³ hybridized carbons over the total carbon count of the molecule, MR – molar refractivity, TPSA – topological polar surface area (Å²).

teolytic cleavage is mediated by the major protease (M^{Pro}) also known as 3-chymotrypsin-like protease (3CL^{Pro}) and by papain-like protease (PL^{Pro}). M^{Pro} is homodimeric cysteine protease which cleaves the polyprotein at 11 different locations creating essential proteins for the viral life cycle. This functional significance of M^{Pro} in the viral life cycle, together with the absence of closely linked homologues in humans, makes the M^{Pro} an attractive target for Covid-19 antiviral drug discovery [17] (Figure 3).

Literature review showed, that all selected phytoconstituents possess potent antiviral potential but not screened against SARS-CoV-2. This is the first attempt to check the potential of selected phytoconstituents against SARS-CoV-2 by docking on two M^{Pro} proteins.

METHODS

Selection of phytoconstituents

22 phytoconstituents were selected based on a review of literature from IMPPAT 2.0 database containing information from more than 100 books on traditional Indian medicine, 7000+ published research articles, and other

resources. The database offers information regarding the phytochemicals, medicinal applications, 2D and 3D chemical structures in order to screen virtually the capacity of phytocandidates to bind at spike protein. The phytoconstituents were selected based on their antiviral effects. Table 3 shows the phytoconstituents selected for the study with their IMPPAT-ID.

Prediction of ADMET analysis

For the purpose of estimating each ADME analyses (physicochemical properties, water solubility, lipophilicity, pharmacokinetics, drug similarity, and medicinal chemistry), the Swiss Institute of Bioinformatics' SwissADME software (www.swissadme.ch) was utilised. The lipophilic characteristics were classified into three broad categories: fragmental (wLog *P*, based on fragments), topological (mLog *P*, based on descriptors), and 3D physics-based (iLog *P* and xLog *P*, based on solvent-free energy in octanol). The pink area represents the optimal range for each property (lipophilicity: MLOGP less than 4.15, XLOGP between -0.7 and +5.0, size: MW between 150 and 500 g/mol, polarity: TPSA between 20

Table 6. Water solubility profile of selected phytocandidates

Molecule name	Log S (ESOL)	Solubility	Class	Log S (Ali)	Solubility	Class	Log S (SILICOS-IT)	Solubility	Class
Artemisinin	-3.42	1.08e ⁻⁰¹ mg/ml 3.82e ⁻⁰⁴ mol/l	Soluble	-3.69	5.71e ⁻⁰² mg/ml 2.02e ⁻⁰⁴ mol/l	Soluble	-2.03	2.61e ⁺⁰⁰ mg/ml 9.25e ⁻⁰³ mol/l	Soluble
Niranthin	-4.59	1.12e ⁻⁰² mg/ml 2.59e ⁻⁰⁵ mol/l	Moderately soluble	-5.14	3.12e ⁻⁰³ mg/ml 7.21e ⁻⁰⁶ mol/l	Moderately soluble	-6.91	5.27e ⁻⁰⁵ mg/ml 1.22e ⁻⁰⁷ mol/l	Poorly soluble
Phylltetralin	-4.50	1.32e ⁻⁰² mg/ml 3.17e ⁻⁰⁵ mol/l	Moderately soluble	-4.63	9.85e ⁻⁰³ mg/ml 2.36e ⁻⁰⁵ mol/l	Moderately soluble	-6.82	6.38e ⁻⁰⁵ mg/ml 1.53e ⁻⁰⁷ mol/l	Poorly soluble
Astragalinalin	-3.18	2.97e ⁻⁰¹ mg/ml 6.61e ⁻⁰⁴ mol/l	Soluble	-4.29	2.28e ⁻⁰² mg/ml 5.08e ⁻⁰⁵ mol/l	Moderately soluble	-2.10	3.55e ⁺⁰⁰ mg/ml 7.91e ⁻⁰³ mol/l	Soluble
5-Hydroxy-3,7,8,3',4'-pentamethoxyflavone	-4.44	1.40e ⁻⁰² mg/ml 3.61e ⁻⁰⁵ mol/l	Moderately soluble	-5.15	2.75e ⁻⁰³ mg/ml 7.09e ⁻⁰⁶ mol/l	Moderately soluble	-6.12	2.92e ⁻⁰⁴ mg/ml 7.52e ⁻⁰⁷ mol/l	Poorly soluble
Secologanin	-0.70	7.76e ⁺⁰¹ mg/ml 2.00e ⁻⁰¹ mol/l	Very soluble	-1.06	3.37e ⁺⁰¹ mg/ml 8.68e ⁻⁰² mol/l	Very soluble	1.30	7.78e ⁺⁰³ mg/ml 2.00e ⁺⁰¹ mol/l	Soluble
Apigenin	-3.94	3.07e ⁻⁰² mg/ml 1.14e ⁻⁰⁴ mol/l	Soluble	-4.59	6.88e ⁻⁰³ mg/ml 2.55e ⁻⁰⁵ mol/l	Moderately soluble	-4.40	1.07e ⁻⁰² mg/ml 3.94e ⁻⁰⁵ mol/l	Moderately soluble
Withaferin A	-4.97	5.01e ⁻⁰³ mg/ml 1.07e ⁻⁰⁵ mol/l	Moderately soluble	-5.55	1.33e ⁻⁰³ mg/ml 2.82e ⁻⁰⁶ mol/l	Moderately soluble	-3.79	7.54e ⁻⁰² mg/ml 1.60e ⁻⁰⁴ mol/l	Soluble
Eugenol	-2.46	5.69e ⁻⁰¹ mg/ml 3.47e ⁻⁰³ mol/l	Soluble	-2.53	4.90e ⁻⁰¹ mg/ml 2.98e ⁻⁰³ mol/l	Soluble	-2.79	2.65e ⁻⁰¹ mg/ml 1.61e ⁻⁰³ mol/l	Soluble
Curcumin	-3.94	4.22e ⁻⁰² mg/ml 1.15e ⁻⁰⁴ mol/l	Soluble	-4.83	5.50e ⁻⁰³ mg/ml 1.49e ⁻⁰⁵ mol/l	Moderately soluble	-4.45	1.31e ⁻⁰² mg/ml 3.56e ⁻⁰⁵ mol/l	Moderately soluble
Citronellic acid	-2.47	5.79e ⁻⁰¹ mg/ml 3.40e ⁻⁰³ mol/l	Soluble	-3.47	5.79e ⁻⁰² mg/ml 3.40e ⁻⁰⁴ mol/l	Soluble	-1.76	2.94e ⁺⁰⁰ mg/ml 1.73e ⁻⁰² mol/l	Soluble
Quercetin	-3.16	2.11e ⁻⁰¹ mg/ml 6.98e ⁻⁰⁴ mol/l	Soluble	-3.91	3.74e ⁻⁰² mg/ml 1.24e ⁻⁰⁴ mol/l	Soluble	-3.24	1.73e ⁻⁰¹ mg/ml 5.73e ⁻⁰⁴ mol/l	Soluble
Rosmarinic acid	-3.44	1.31e ⁻⁰¹ mg/ml 3.63e ⁻⁰⁴ mol/l	Soluble	-5.04	3.32e ⁻⁰³ mg/ml 9.22e ⁻⁰⁶ mol/l	Moderately soluble	-2.17	2.41e ⁺⁰⁰ mg/ml 6.70e ⁻⁰³ mol/l	Soluble
Carvacrol	-3.31	7.40e ⁻⁰² mg/ml 4.92e ⁻⁰⁴ mol/l	Soluble	-3.60	3.79e ⁻⁰² mg/ml 2.53e ⁻⁰⁴ mol/l	Soluble	-3.01	1.46e ⁻⁰¹ mg/ml 9.71e ⁻⁰⁴ mol/l	Soluble
Ingenol	-2.07	2.99e ⁺⁰⁰ mg/ml 8.58e ⁻⁰³ mol/l	Soluble	-1.83	5.19e ⁺⁰⁰ mg/ml 1.49e ⁻⁰² mol/l	Very soluble	-1.63	8.22e ⁺⁰⁰ mg/ml 2.36e ⁻⁰² mol/l	Soluble
Calanolide B	-4.70	7.43e ⁻⁰³ mg/ml 2.00e ⁻⁰⁵ mol/l	Moderately soluble	-4.98	3.85e ⁻⁰³ mg/ml 1.04e ⁻⁰⁵ mol/l	Moderately soluble	-5.70	7.43e ⁻⁰⁴ mg/ml 2.00e ⁻⁰⁶ mol/l	Moderately soluble
β-Amyrin	-8.25	2.40e ⁻⁰⁶ mg/ml 5.62e ⁻⁰⁹ mol/l	Poorly soluble	-9.47	1.44e ⁻⁰⁷ mg/ml 3.38e ⁻¹⁰ mol/l	Poorly soluble	-7.16	2.93e ⁻⁰⁵ mg/ml 6.85e ⁻⁰⁸ mol/l	Poorly soluble
β-Caryophyllene	-3.87	2.78e ⁻⁰² mg/ml 1.36e ⁻⁰⁴ mol/l	Soluble	-4.10	1.64e ⁻⁰² mg/ml 8.01e ⁻⁰⁵ mol/l	Moderately soluble	-3.77	3.49e ⁻⁰² mg/ml 1.71e ⁻⁰⁴ mol/l	Soluble
Oleanolic acid	-7.32	2.16e ⁻⁰⁵ mg/ml 4.74e ⁻⁰⁸ mol/l	Poorly soluble	-8.53	1.34e ⁻⁰⁶ mg/ml 2.94e ⁻⁰⁹ mol/l	Poorly soluble	-6.12	3.45e ⁻⁰⁴ mg/ml 7.55e ⁻⁰⁷ mol/l	Poorly soluble /s
Cucurbitacin D	-4.08	4.33e ⁻⁰² mg/ml 8.37e ⁻⁰⁵ mol/l	Moderately soluble	-4.46	1.78e ⁻⁰² mg/ml 3.44e ⁻⁰⁵ mol/l	Moderately soluble	-3.66	1.13e ⁻⁰¹ mg/ml 2.18e ⁻⁰⁴ mol/l	Soluble
Kuwanon L	-6.99	6.45e ⁻⁰⁵ mg/ml 1.03e ⁻⁰⁷ mol/l	Poorly soluble	-9.14	4.51e ⁻⁰⁷ mg/ml 7.20e ⁻¹⁰ mol/l	Poorly soluble	-6.30	3.13e ⁻⁰⁴ mg/ml 4.99e ⁻⁰⁷ mol/l	Poorly soluble
Patentiflorin A	-4.55	1.49e ⁻⁰² mg/ml 2.84e ⁻⁰⁵ mol/l	Moderately soluble	-4.95	5.93e ⁻⁰³ mg/ml 1.13e ⁻⁰⁵ mol/l	Moderately soluble	-4.95	5.92e ⁻⁰³ mg/ml 1.12e ⁻⁰⁵ mol/l	Moderately soluble

and 130 Å², solubility: log S not higher than 6, saturation: the fraction of carbons in the sp³ hybridization not less than 0.25, and flexibility: no more than 9 rotatable bonds). From these results, the compound can be predicted not as orally bioavailable, but as too flexible and polar. The perceptive evaluation of passive gastrointestinal absorption (HIA) and brain penetration (BBB) with molecules in the WLOGP-versus-TPSA is shown in BOILED-Egg (Egan Egg) (Figure 4) [40]. The yellow part of the boiled egg shows the lipophilic drugs, which can

cross the blood-brain barrier (BBB), drugs in the eclipsed part are 90% absorbed, and drugs outside the eclipsed are 30% absorbed.

Hardware and software

The computational inquiry was carried out using Windows 10 (64-bit) operating systems with 8 GB RAM and 2.11 GHz Intel® Core™ i5-10210U processor. The Scripps Research Institute's PyRx python prescription

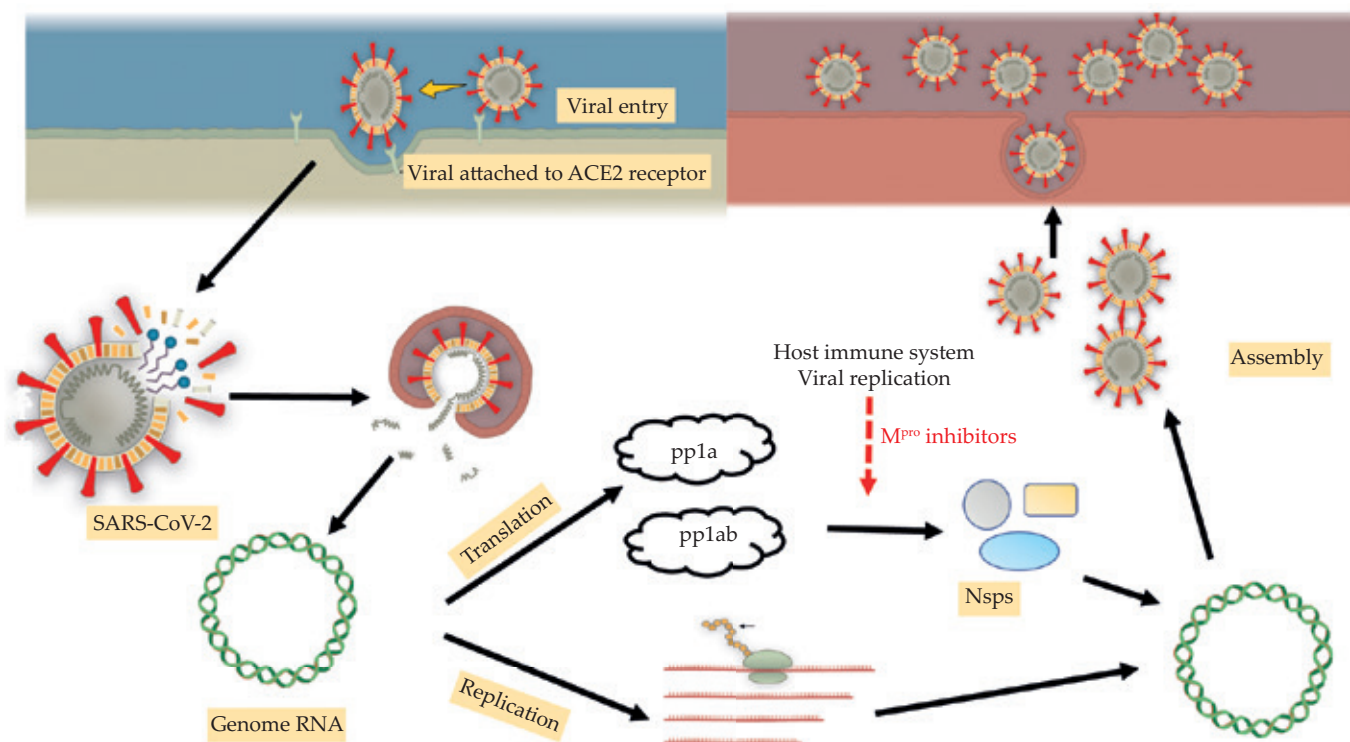


Fig. 5. Mechanism of M^{pro} inhibitors (Orf 1a/1b gene product is referred to as polyprotein 1a or pp1a)

0.8 binary package for Windows is available for free at <https://pyrx.sourceforge.io/downloads>.

Protein preparation

Before performing any computations, the system must be thoroughly picked and readied. The initial step is to get a protein structure, preferably one that has a bound ligand. In this study, M^{pro} inhibitors were selected. M^{pro} is responsible for processing the remaining non-structural proteins of SARS coronaviruses as shown in Figure 5 [41]. 3D structures with excellent resolution, as well as structures co-crystallized with high-affinity ligands or natural substrates, were particularly suggested [42]. The M^{pro} proteins 6LU7 (complex with an inhibitor N3) and 5C3N (space group C2221) were retrieved from the RCSB database PDB (Protein Data Bank) and employed in docking research (Figure 6) [43]. Using the Autodock Tool, the protein structure was examined and modified, and missing residues around the active site were inserted [44, 45]. To prepare, conduct, and evaluate docking simulations, the Autodock tools graphical user interface application was employed. Kollman unified atom charges, solvation parameters, and polar hydrogen were introduced to the receptor for protein construction in docking simulation. Because ligands are not peptides, the Gasteiger charge was assigned first, followed by the addition of non-polar hydrogens. Autodock comes with pre-calculated grid charts, one for each kind of atom, that show the docked ligand as it stores the potential

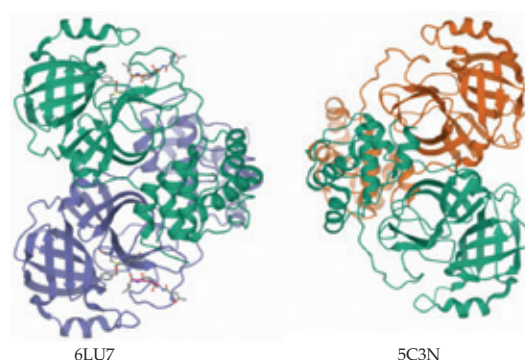


Fig. 6. 3D structure of proteins 6LU7 and 5C3N

energy. This grid must encompass the area of interest (active site) in the macromolecule [46]. Geometry was used to improve the protein-ligand combination using the UFF force field [47].

Ligands preparation

Chemdraw Created was used to draw the ligand structures, and Open Babel in PyRx was used to do energy reduction using UFF (universal force field).

RESULTS AND DISCUSSION

The protein preparation and all the docking results from Autodock were reposed by using discovery studio and shown in Figs. 7, 8, 10, 11, 13, 14, and 15.

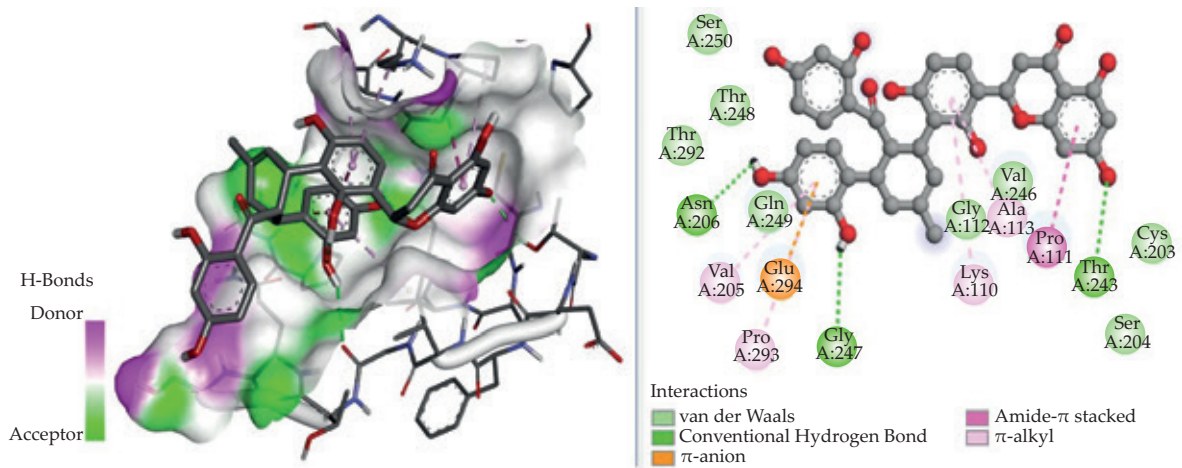


Fig. 7. 3D & 2D binding conformation of kuwanon L-5C3N at the active site of spike protein

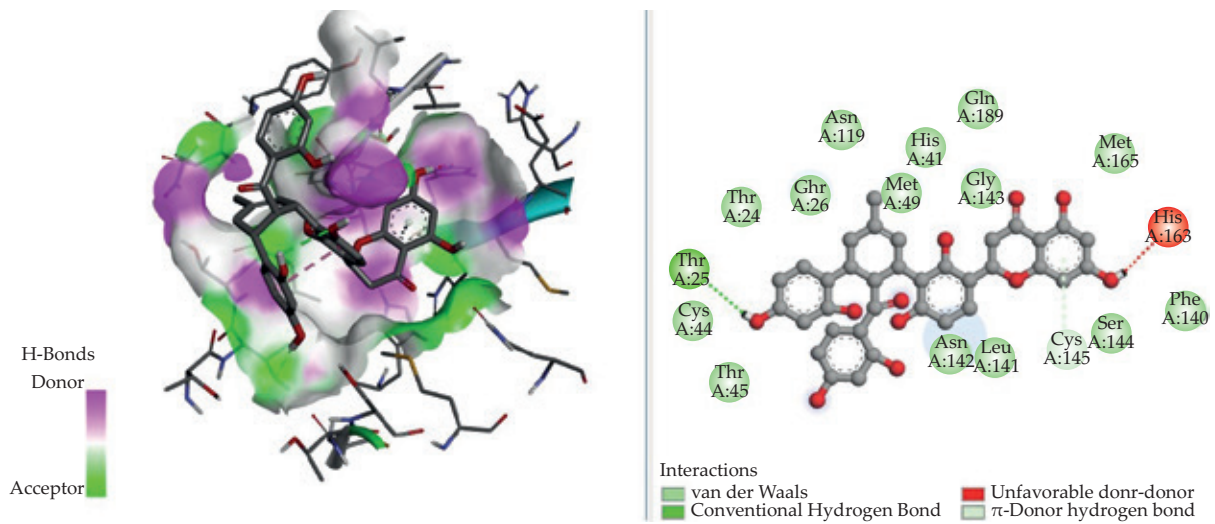


Fig. 8. 3D & 2D binding conformation of kuwanon L-6LU7 at the active site of spike protein

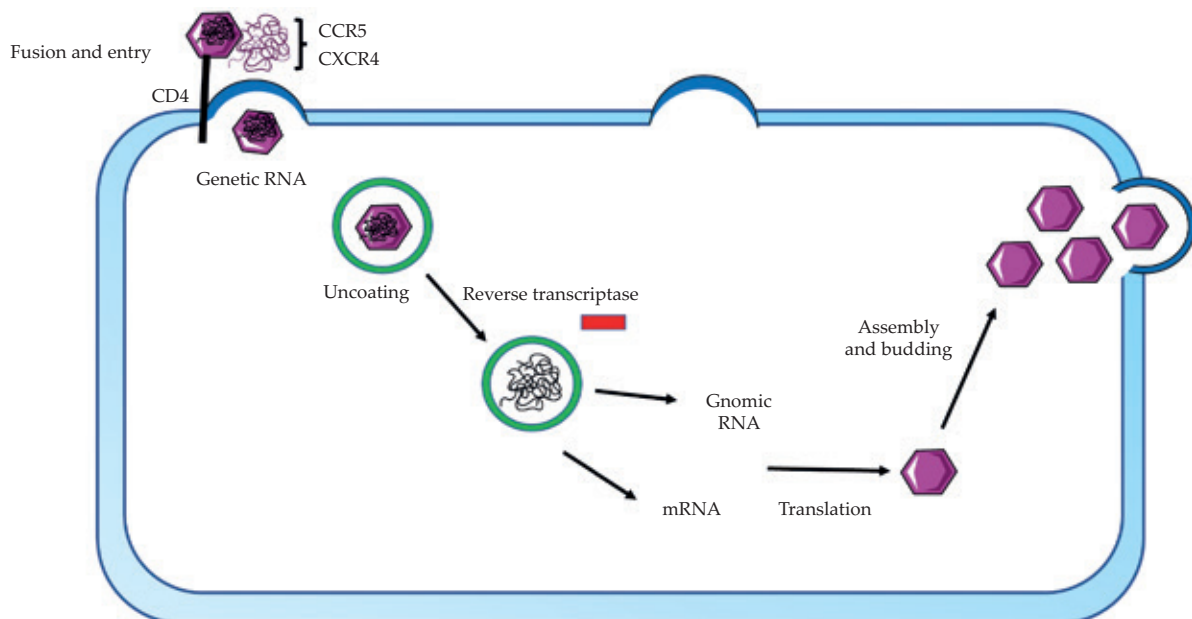


Fig. 9. Antiviral activity of kuwanon L

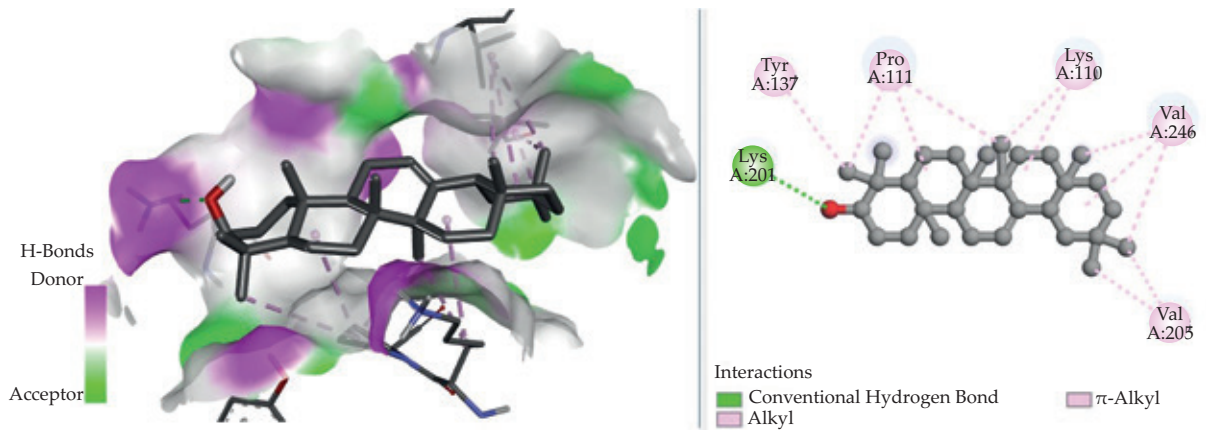


Fig. 10. 3D & 2D binding conformation of β -amyrin-5C3N at the active site of spike protein

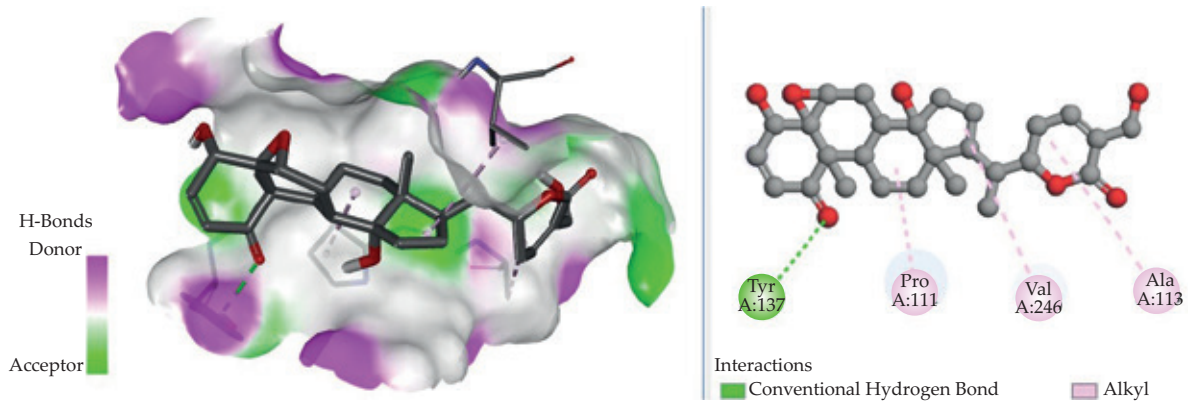


Fig. 11. 3D & 2D binding conformation of withaferin A-5C3N at the active site of spike protein

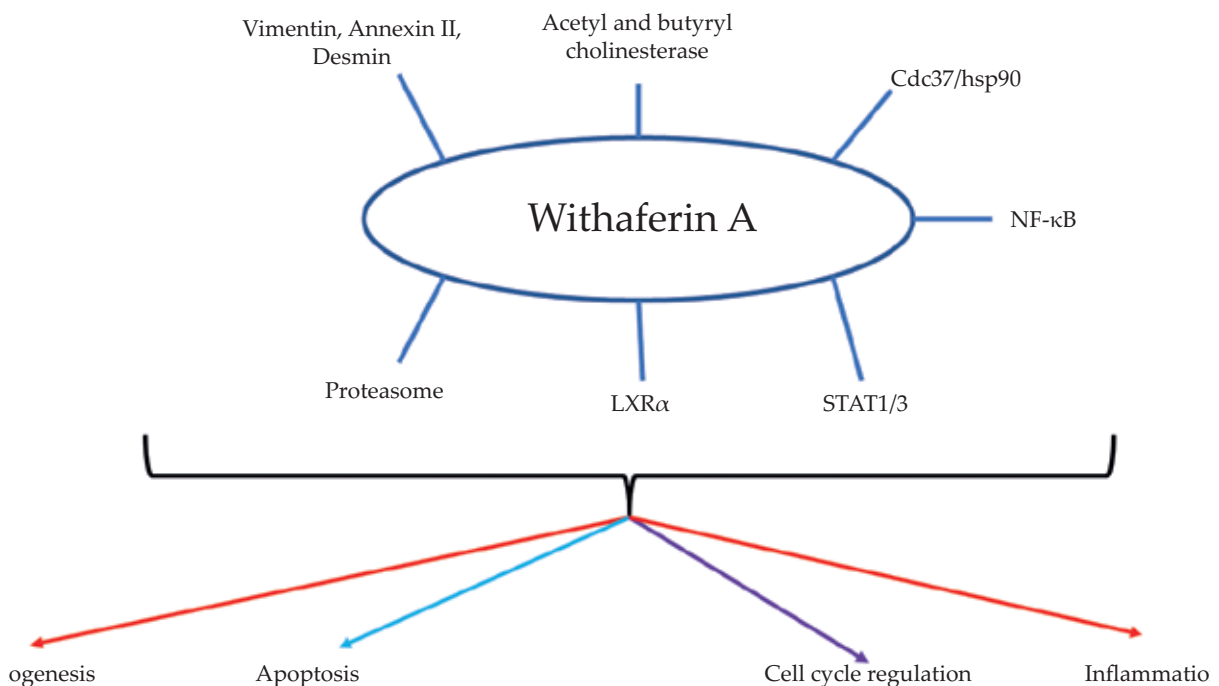


Fig. 12. Role of withaferin A in various disorders

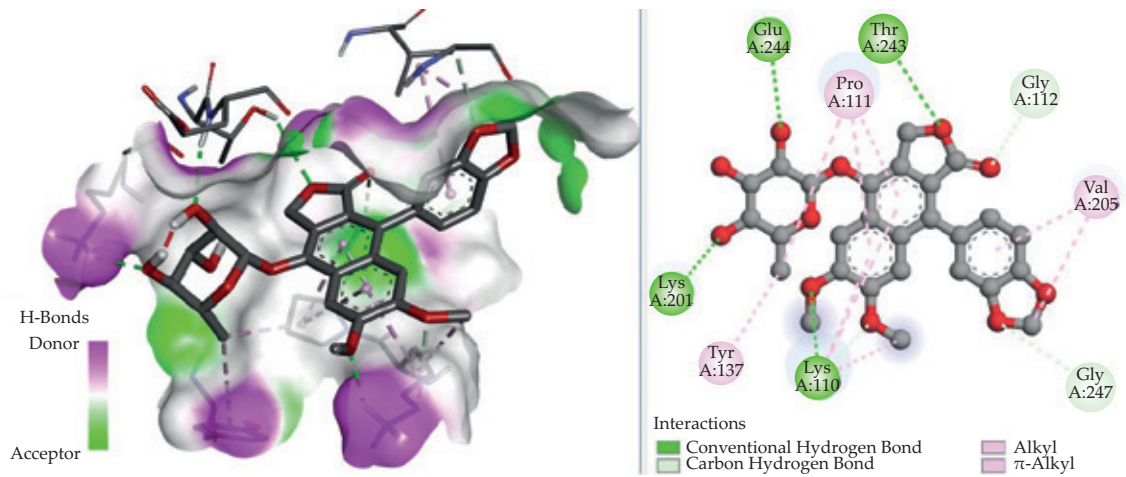


Fig. 13. 3D & 2D binding conformation of patentiflorin A-5C3N at the active site of spike protein

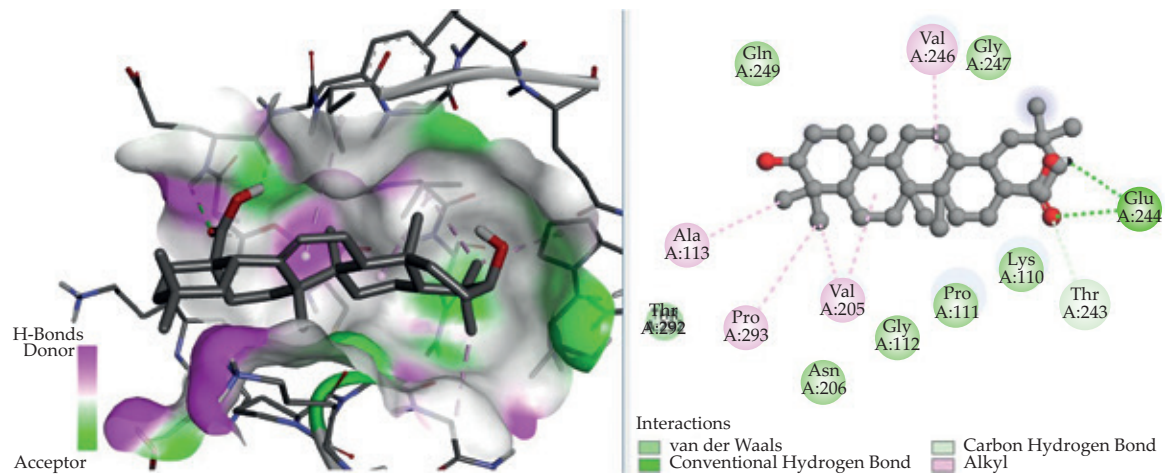


Fig. 14. 3D & 2D binding conformation of oleanolic acid-5C3N at the active site of spike protein

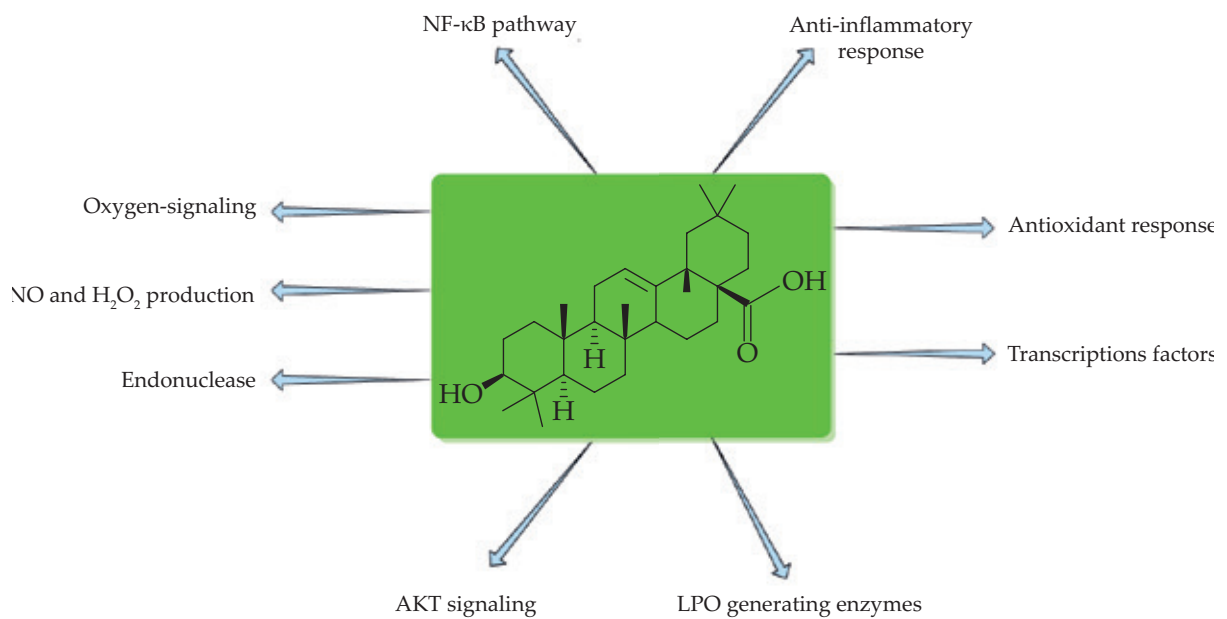


Fig. 15. Mechanism of action of oleanolic acid

Table 7. Pharmacokinetics of selected phytocandidates

Molecule name	GI absorption	BBB permeant	P-gp substrate	CYP1A2 inhibitor	CYP2C19 inhibitor	CYP2C9 inhibitor	CYP2D6 inhibitor	CYP3A4 inhibitor	Log K_p (skin permeation) cm/s
Artemisinin	High	Yes	No	Yes	No	No	No	No	-5.96
Niranthin	High	Yes	No	No	No	No	Yes	Yes	-6.04
Phlytetralin	High	Yes	No	No	No	No	Yes	Yes	-6.16
Astragalinalin	Low	No	No	No	No	No	No	No	-8.52
5-Hydroxy-3,7,8,3',4'-pentamethoxyflavone	High	No	No	No	No	Yes	No	Yes	-6.23
Secologanin	Low	No	No	No	No	No	No	No	-9.82
Apigenin	High	No	No	Yes	No	No	Yes	Yes	-5.80
Withaferin A	High	No	Yes	No	No	No	No	No	-6.45
Eugenol	High	Yes	No	Yes	No	No	No	No	-5.69
Curcumin	High	No	No	No	No	Yes	No	Yes	-6.28
Citronellic acid	High	Yes	No	No	No	No	No	No	-5.19
Quercetin	High	No	No	Yes	No	No	Yes	Yes	-7.05
Rosmarinic acid	Low	No	No	No	No	No	No	No	-6.28
Carvacrol	High	Yes	No	Yes	No	No	No	No	-4.74
Ingenol	High	No	Yes	No	No	No	No	No	-8.28
Calanolide B	High	Yes	Yes	No	Yes	Yes	Yes	Yes	-5.83
β -Amyrin	Low	No	No	No	No	No	No	No	-2.41
β -Caryophyllene	Low	No	No	No	Yes	Yes	No	No	-4.44
Oleanolic acid	Low	No	No	No	No	No	No	No	-3.77
Cucurbitacin D	High	No	Yes	No	No	No	No	No	-7.99
Kuwanon L	Low	No	No	No	No	No	No	No	-6.51
Patentiflorin A	Low	No	No	No	No	Yes	Yes	Yes	-7.86

CYP1A2 – cytochrome P450 family 1 subfamily A member 2 (PDB:2HI4), CYP2C19 – cytochrome P450 family 2 subfamily C member 19 (PDB:4GQS), CYP2C9 – cytochrome P450 family 2 subfamily C member 9 (PDB:1OG2), CYP2D6 – cytochrome P450 family 2 subfamily D member 6 (PDB:5TFT), CYP3A4 – cytochrome P450 family 3 subfamily A member 4 (PDB:4K9T).

SwissDock software

The results for ADMET obtained by using SwissDock software are shown in Tables 4–8. The bioavailability score as shown in Table 8 was in the range of 0.11 to 0.85, which was low for secologanin, kuwanon L, and patentiflorin A, whereas highest for citronellic acid. Furthermore, maximum of the phytochemicals studied were shown to be absorbed in the gastrointestinal system as shown in Table 7 except astragalinalin, secologanin, rosmarinic acid, β -caryophyllene, oleanolic acid, kuwanon L, and patentiflorin A. Only 7 out of 22 phytochemicals were capable of crossing the blood-brain barrier, *i.e.*, artemisinin, niranthin, phlytetralin, eugenol, citronellic acid, carvacrol, and calanolide B (Table 7). The consensus Log P_{ow} (indicator of lipophilicity) ranged from -0.95 to 7.18 (Table 5), whereas TPSA (topological polar surface area) ranged from 0 to 205.21 Å² (Table 4). β -Amyrin and oleanolic acid are highly lipophilic as shown in Table 5. Furthermore, withaferin A, ingenol, calanolide B, and cucurbitacin D showed glycoprotein substrate permeability (P-gp) (Table 7). Phytochemicals artemisinin, apigenin, eugenol, quercetin, and carvacrol interacted with

the CYP1A2 isoenzyme of the cytochrome P family, imparting efficacy with low harm (Table 7). Calanolide B interacted with all the cytochromes except CYP1A2 isoenzyme. The bioavailability radar plots of the examined phytochemicals ranged from 0.11 (secologanin) to 0.85 (citronellic acid). Furthermore, the BOILED-Egg graph of thymol, carvacrol, and cinnamaldehyde emerged with a red point within the yellow zone (yolk), suggesting brain penetrability of phytochemicals artemisinin, niranthin, phlytetralin, citronellic acid, carvacrol, and calanolide B. Artemisinin, astragalinalin, secologanin, withaferin A, eugenol, citronellic acid, quercetin, carvacrol, ingenol, and cucurbitacin D are water soluble drugs as shown in Table 6. Among all the selected 22 drugs, astragalinalin, kuwanon L, and patentiflorin A does not follow the Lipinski Rule of 5.

Structure-based virtual screening for docking (6LU7-M^{Pro} and 5C3N-M^{Pro})

The PyRx Autodock wizard application was used as the docking engine for all chemical libraries' molecular docking. The ligands were called flexible throughout the dock-

Table 8. Drug likeness of selected phytocandidates

Molecule name	Lipinski	Ghose	Veber	Egan	Muegge	Bioavailability Score
Artemisinin	Yes	Yes	Yes	Yes	Yes	0.55
Niranthin	Yes	Yes	Yes	Yes	Yes	0.55
Phyltetralin	Yes	Yes	Yes	Yes	Yes	0.55
Astragalin	No	Yes	No	No	No	0.17
5-Hydroxy-3,7,8,3',4'-pentamethoxyflavone	Yes	Yes	Yes	Yes	Yes	0.55
Secologanin	Yes	No	No	No	No	0.11
Apigenin	Yes	Yes	Yes	Yes	Yes	0.55
Withaferin A	Yes	No	Yes	Yes	Yes	0.55
Eugenol	Yes	Yes	Yes	Yes	No	0.55
Curcumin	Yes	Yes	Yes	Yes	Yes	0.55
Citronellic acid	Yes	Yes	Yes	Yes	No	0.85
Quercetin	Yes	Yes	Yes	Yes	Yes	0.55
Rosmarinic acid	Yes	Yes	No	No	Yes	0.56
Carvacrol	Yes	No	Yes	Yes	No	0.55
Ingenol	Yes	Yes	Yes	Yes	Yes	0.55
Calanolide B	Yes	Yes	Yes	Yes	Yes	0.55
β -Amyrin	Yes	No	Yes	No	No	0.55
β -Caryophyllene	Yes	Yes	Yes	Yes	No	0.55
Oleanolic acid	Yes	No	Yes	No	No	0.85
Cucurbitacin D	Yes	No	Yes	No	Yes	0.55
Kuwanon L	No	No	No	No	No	0.17
Patentiflorin A	No	No	No	No	No	0.17

ing process, whereas the protein was supposed to be stiff. The grid configuration file was created in PyRx using the grid box for 6LU7 and 5C3N ($x = -12.49$, $y = 13.94$, $z = 67.57$) [48]. Using Open Babel, we were able to reduce the energy of all chemicals [49]. The Autodock wizard was used to finish the molecular docking [42]. The software was also used to anticipate which amino acids interact with ligands in the protein's active site. The findings of less than 2.0 in positional root-mean-square deviation (RMSD) were judged to be ideal and grouped to identify the favorable binding. The ligand with the highest binding energy was identified as having the highest binding affinity. All of these chemicals' interactions with the Covid-19 major protease might be used to find hits later. Tables 9 and 10 shows how phytoconstituents interact with the 6LU7 and 5C3N proteins, as well as protein binding and G score. Docking results showed that phytoconstituents β -amyryn (-8.4 kcal/mol), withaferin A (-8.3 kcal/mol), oleanolic acid (-7.8 kcal/mol), and patentiflorin A (-8.1 kcal/mol) have shown best results against 5C3N M^{Pro} whereas kuwanon L (-7.1 kcal/mol), β -amyryn (-6.9 kcal/mol), oleanolic acid (-6.8 kcal/mol), cucurbitacin D (-6.5 kcal/mol), and quercetin (-6.5 kcal/mol) against 6LU7 M^{Pro} protein.

DISCUSSION

M^{Pro} is one of the most well-studied pan pharmacological targets in the coronavirus family. M^{Pro} is a critical enzyme for virus endurance since it processes the polyproteins that are translated from viral RNA. The M^{Pro} cleaves all 11 cleavage sites (after a glutamine residue) of polypeptide sequences on the big polyprotein known as 1ab (replicase 1-ab, 790 kDa) during translation; blocking the activity of this enzyme would stop viral replication. At most locations, the cleavage site identification sequence is Leue Gln (Ser, Ala, Gly). There are no human proteases with similar cleavage site selectivity that we are aware of, therefore such inhibitors are unlikely to be hazardous. The M^{Pro} of 6LU7 with 22 phytoconstituents possessing substantial antiviral screening was studied utilizing several docking procedures of Discovery studio and Auto Dock Vina. The results showed that 6 phytocandidates were found to possess better binding affinity and a stronger H-bond with the M^{Pro} of the SARS-CoV-2 binding site than the native N3 peptide.

Table 9. 6LU7 binding energy, H-bond and protein ligand interactions with phytoconstituents

Phytoconstituent	6LU7 binding energy, kcal/mol	H-Bond interaction	Protein ligand interaction
Artemisinin	-5.9	Gly143; His41	Gly143; His41; Ser44; Asn142; Leu141; Met165; His164; Glu166; Gln189; Met49; Thr25; Thr26; Cys145; Leu27
Niranthin	-5	Gly143	Gly143; Asn142; Ser144; Met49; Thr25
Phyltetralin	-5.9	Cys145	Cys145; Thr45; Met49; Asn142; Leu141
β -Amyrin	-6.9	–	Met165; Cys145; Met49; His41
Astragalinalin	-6.4	Ser46; Gly143; Cys145	Ser46; Gly143; Cys145
5-Hydroxy-3,7,8,3',4'-pentamethoxyflavone	-5.9	Ser46; Thr26; Thr24	Ser46; Met49; Cys145; His41; His163; Thr26; Thr24
Secologanin	-5.4	His41; Thr24; Cys44	His41; Met49; Thr24; Cys44
Apigenin	-6.8	Leu141; Gly143	Leu141; Gly143; Cys143; His41; Met49; Thr25
Withaferin A	-6.3	Ser46; Gly143	Thr45; Ser46; Gly143
Eugenol	-4.4	Gly143; Asp187; Ser46	Gly143; His41; His164; Met165; Asp187; Met49; Ser46
Curcumin	-6.1	Gly143; Asp187; Ser46	His41; His164; Met165; Met49; Gly143; Asp187; Ser46
Citronellic acid	-4.8	–	Leu141; Met165; Met49; Cys145; His41
Quercetin	-6.5	His164; Thr26; Gly143	Cys145; His164; Thr26; Gly143
Rosmarinic acid	-6.1	Ser46; Cys145; Ser144; Leu141; Gly143	Ser46; Cys145; Ser144; Leu141; Gly143
Carvacrol	-4.6	Cys145; Leu141; Ser144	His41; Gly143; Cys145; Leu141; Ser144
β -Caryophyllene	-5	–	Leu27; His41; Cys145
Oleanolic acid	-6.8	Leu141	His41; Cys145; Ser144; Met49; Leu141
Cucurbitacin D	-6.5	Asn65; Gly23; Cys22; Thr24; Cys44	Leu67; Asn65; Gly23; Cys22; Thr24; Cys44
Calanolide B	-5.6	–	His41; Leu27; Cys145; Gly143; Thr26
Ingenol	-5.7	Ser46; Thr25	Leu27; Met49; Cys145; His41; Ser46; Thr25
Kuwanon L	-7.1	Thr25	Thr25; Thr24; Thr26; Asn119; Met49; His41; Gln189; Gly143; Met165; His163; Phe140; Ser144; Cys145; Leu141; Asn142; Thr45; Cys44
Patentiflorin A	-6.4	Thr24; Thr26; His41	Met165; Met49; Thr24; Thr26; His41

Kuwanon L

Kuwanons are derived from the root bark of *Morus alba*, a tree in the *Moraceae* family that has the potential to treat allergy conditions by inhibiting histamine release. Kuwanon G did not substantially reduce 5-LO activation in PMA and A23187-stimulated MC/9 mast cells, but it did not block LTC₄ synthesis. Kuwanon L outperformed the other 22 drugs in terms of docking scores against both the 5C3N (Figure 7) and 6LU7 (Figure 8) receptors. Thr25; Thr24; Thr26; Asn119; Met49; His41; Gln189; Gly143; Met165; His163; Phe140; Ser144; Cys145; Leu141; Asn142; Thr45; Cys44; Thr45; Cys44; Thr45; Cys44; Thr45; Cys44; Thr45; Cys44; Thr45; Cys44; Thr45; Cys44 [50].

Kuwanon L has shown promise against HIV because it inhibits the reverse transcriptase enzyme, which is necessary for RNA virus replication. As shown in Figure 9, an antiviral activity that has shown optimal binding

to both spike proteins of SARS-CoV-2 virus may act as a potential lead molecule for future therapy development against SARS-CoV-2 virus [51].

β -Amyrin

The top docking posture compound is β -amyrin, which had a 5C3N-G score of -8.4 kcal/mol and has significant binding sites of Lys201; Tyr137; Pro111; Lys110; Val246; Val205, and an H-bond interaction with Lys201 (Figure 10). β -Amyrin is a plant-derived triterpenoid skeleton that has a wide range of uses in the food and medicinal industries. It is also a precursor of oleanolic acid, which has a high binding and docking score. On LPS-induced hPBMCs, β -amyrin was found to suppress PGE₂, IL-6 release, and NF- κ B activation in a concentration-dependent manner. As a result, β -amyrin might be a viable and growing platform for treating a variety of inflammatory illnesses [52].

Table 10. 5C3N binding energy, H-bond and protein ligand interactions with phytoconstituents

Phytoconstituent	5C3N binding energy, kcal/mol	H-Bond interaction	Protein ligand interaction
Artemisinin	-6.3	–	Lys110; Ala113; Pro193; Val205
Niranthin	-6.7	Lys201; Thr243	Lys201; Thr243; Pro135; Glu244; Val246; Val205; Ala113; Pro111
Phyltetralin	-5.8	–	Glu294; Val205; Cys203; Val109; Ala113; Lys110
β-Amyrin	-8.4	Lys201	Lys201; Tyr137; Pro111; Lys110; Val246; Val205
Astragaln	-6.8	Glu294; Gly247	Thr243; Pro111; Val246; Lys110; Glu294; Gly247
5-Hydroxy-3,7,8,3',4'-pentamethoxyflavone	-6.1	–	Ala113; Pro111; Lys110; Val205; Glu294
Secologanin	-5.1	Glu244; Tyr137	Thr243; Gly112; Pro135; Pro111; Glu244; Tyr137
Apigenin	-7.0	Glu294	Pro293; Ala113; Val205; Pro111; Cys203; Glu294
Withaferin A	-8.3	Tyr237	Pro111; Val246; Ala113; Tyr237
Eugenol	-4.5	–	Glu294; Ala113; Val205
Curcumin	-7.0	Thr243; Tyr137; Glu294	Pro135; Pro111; Ala113; Val205; Thr243; Tyr137; Glu294
Citronellic acid	-4.9	Thr130; Ala144	Ala113; His108; Met298; Phe115; Thr130; Ala144
Quercetin	-7.1	Gly112; Gln249	Val205; Pro111; Lys110; Thr243; Gly112; Gln249
Rosmarinic acid	-7.1	Glu244; Gly112; Asn206; Gln249	Val205; Thr243; Pro111; Pro135; Glu244; Gly112; Asn206; Gln249
Carvacrol	-4.9	–	Val205; Pro293
β-Caryophyllene	-5.5	–	Val205; Pro293; Lys110; Val246
Oleanolic acid	-7.8	Glu244	Glu244; Thr243; Lys110; Pro111; Gly112; Val205; Asn206; Pro293; Thr292; Ala113; Gln249; Val246; Gly247
Cucurbitacin D	-7.6	Thr243	Pro111; Tyr137; Val205; Thr243
Calanolide B	-7.1	Thr243	Val205; Ala113; Pro293; Pro111; Val246; Lys110; Thr243
Ingenol	-6.7	Asn206	Cys203; Val205; Val246; Asn206
Kuwanon L	-7.6	Asn206; Thr243; Gly247	Cys203; Ser204; Pro111; Val246; Ala113; Gly112; Lys110; Glu294; Pro293; Gln249; Val205; Thr292; Thr248; Ser250; Asn206; Thr243; Gly247
Patentiflorin A	-8.1	Glu244; Thr243; Lys110; Lys201	Glu244; Pro111; Thr243; Gly112; Val205; Gly247; Lys110; Tyr137; Lys201

Withaferin A

Withaferin A was discovered to have a 5C3N-G score of -8.3 kcal/mol and significant binding sites of Pro111; Val246; Ala113; Tyr237, as well as an H-bond interaction with Tyr237 (Figure 11). Because of its multifaceted biological features, withaferin A (WA) is a crucial withanolide that has carved out a prominent role in study. *Withania somnifera* Dunal has a large amount of it. Ashwagandha (WS) is one of Ayurveda's prehistoric important medicines. Withaferin A is an anti-inflammatory drug that can help fight cancer-related inflammation. It can stop cancer from starting and progressing by targeting molecular markers of inflammation. Inflammation, angiogenesis, metastasis, anti-apoptosis, and multidrug resistance are all triggered by the NF- κ B transcription factor. As seen in Figure 12, NF- κ B activity irregularities contribute to chronic inflammation and, eventually, cancer [53].

Patentiflorin A

Patentiflorin A came in third with a docking score of -8.1 kcal/mol, and its primary binding sites were Glu244; Pro111; Thr243; Gly112; Val205; Gly247; Lys110; Tyr137; Lys201, with H-bonding detected with Glu244; Thr243; Lys110; Lys201 (Figure 13). Patentiflorin A, a potent anti-HIV-1 chemical derived from *Justicia gendarussa* that inhibits reverse transcriptase far more efficiently than the initial HIV medicine zidovudine, might be a promising target for finding an effective anti-SARS-CoV-2 therapy [54].

Oleanolic acid

Oleanolic acid docking score of -7.8 kcal/mol was discovered, with main binding sites Glu244; Thr243; Lys110; Pro111; Gly112; Val205; Asn206; Pro293; Thr292; Ala113; Gln249; Val246; Gly247, among which Glu244 interacts

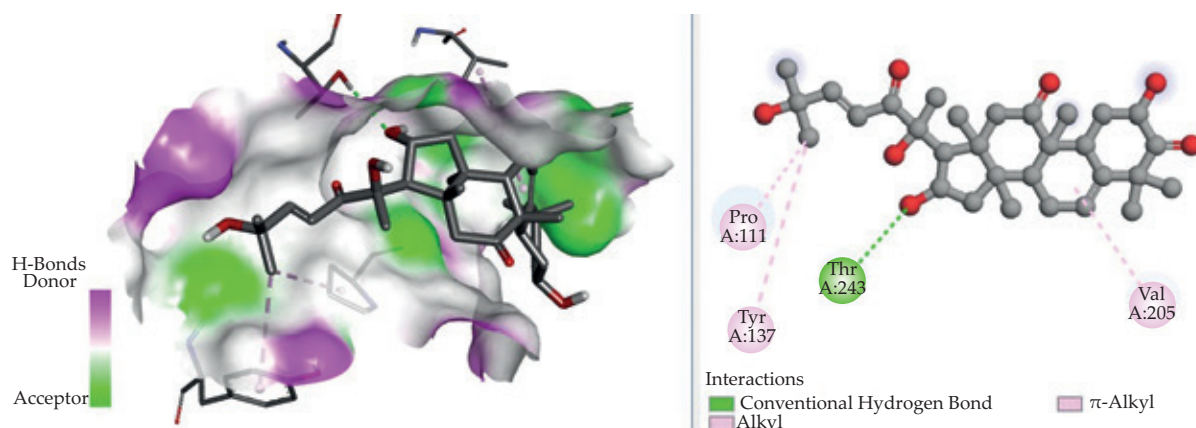


Fig. 16. 3D & 2D binding conformation of cucurbitacin D-5C3N at the active site of spike protein

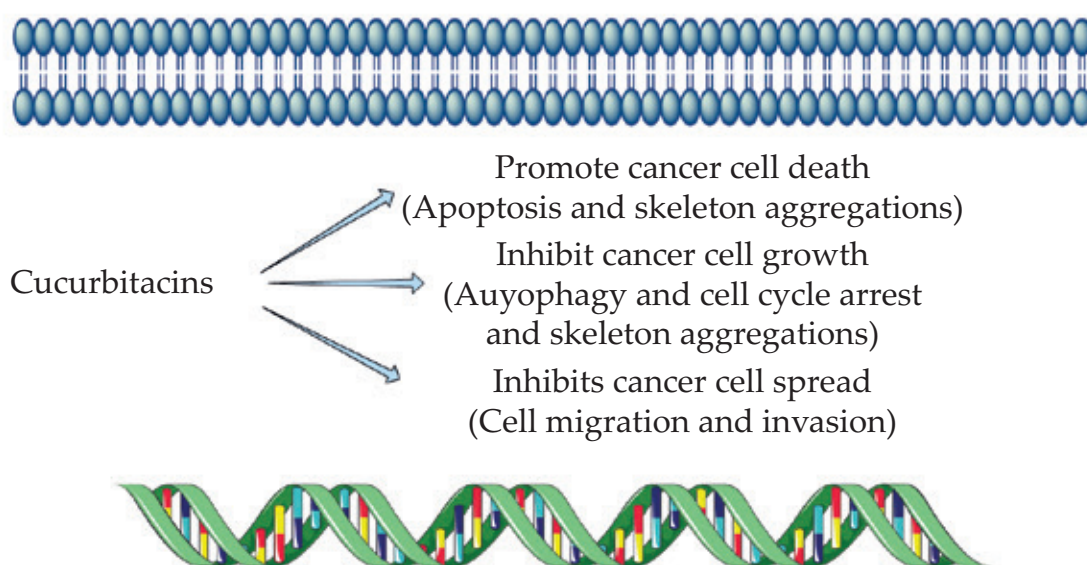


Fig. 17. Mechanism of action of cucurbitacins as anticancer agents

with H-bond, as shown in Figure 14. Oleanolic acids are triterpenoid chemicals found in a wide range of foods, medicinal herbs, and plants. Oleanolic acids, which have been shown to protect against chemically induced liver injury in experimental animals, have been promoted in China as a treatment for human liver problems. The prevention of toxicant activation and the augmentation of the body's defensive mechanisms may be involved in hepatoprotection's mechanism. As shown in Figure 15 [55], oleanolic acids have long been known to have anti-inflammatory and antihyperlipidemic effects.

Cucurbitacins

Cucurbitacin D was found to be the fifth best scorer, with a docking score of -7.6 kcal/mol. Major interaction sites were Pro111; Tyr137; Val205; Thr243, with Thr243 interacting with H-bonding (Figure 16). Cucurbitacins are a multiplex category of various chemicals found not only in the *Cucurbitaceae* family but also in other fami-

lies. Cucurbitacins have anticancer properties because they promote apoptosis, autophagy, cell cycle arrest, and cell migration and invasion inhibition (Figure 17). Cucurbitacin has anti-inflammatory properties through preventing nuclear translocation of NF- κ B p65 [56].

CONCLUSIONS

This study found that natural β -amyrin, oleanolic acid, kuwanon L, and patentiflorin A had high binding free energies with the M^{Pro} and S protein of the SARS-CoV-2 virus. The results are only a preliminary screening to help with future research that will start with tests in vitro, in animal models, or in human clinical trials.

ACKNOWLEDGEMENTS

The authors acknowledge the Dean, Faculty of Pharmacy, IFTM University, Moradabad for providing continuous support for the article.

REFERENCES

- [1] Yan R., Zhang Y., Li Y. *et al.*: *Science* **2020**, 367(6485), 1444.
<https://doi.org/10.1126/science.abb2762>
- [2] Chen Y., Liu Q., Guo D.: *Journal of Medical Virology* **2020**, 92(4), 418.
<https://doi.org/10.1002/jmv.25681>
- [3] Su S., Wong G., Shi W. *et al.*: *Trends in Microbiology* **2016**, 24(6), 490.
<https://doi.org/10.1016/j.tim.2016.03.003>
- [4] Raeiszadeh M., Adeli B.: *ACS Photonics* **2020**, 7(11), 2941.
<https://doi.org/10.1021/acsp Photonics.0c01245>
- [5] Chen L., Li Q., Zheng D. *et al.*: *The New England Journal of Medicine* **2020**, 382(25), e100.
<https://doi.org/10.1056/NEJMc2009226>
- [6] Mousavizadeh L., Ghasemi S.: *Journal of Microbiology, Immunology and Infection* **2021**, 54(2), 159.
<https://doi.org/10.1016/j.jmii.2020.03.022>
- [7] Muratov E.N., Amaro R., Andrade C.H. *et al.*: *Chemical Society Reviews* **2021**, 50(16), 9121.
<https://doi.org/10.1039/D0CS01065K>
- [8] Gordon D.E., Jang G.M., Bouhaddou M. *et al.*: *Nature* **2020**, 583(7816), 459.
<https://doi.org/10.1038/s41586-020-2286-9>
- [9] Sultana A., Tasnim S., Hossain M.M. *et al.*: *F1000Res* **2021**, 10, 81.
<https://doi.org/10.12688/f1000research.50880.1>
- [10] Heller L., Mota C.R., Greco D.B.: *Science of The Total Environment* **2020**, 729, 138919.
<https://doi.org/10.1016/j.scitotenv.2020.138919>
- [11] <https://www.who.int/en/activities/tracking-SARS-CoV-2-variants> (access date: 15.01.2022)
- [12] Galindez G., Matschinske J., Rose T.D. *et al.*: *Nature Computational Science* **2021**, 1, 33.
<https://doi.org/10.1038/s43588-020-00007-6>
- [13] Mohamed N.A., Solehan H.M., Mohd Rani M.D. *et al.*: *PLoS ONE* **2021**, 16(8), e0256110.
<https://doi.org/10.1371/journal.pone.0256110>
- [14] Kwon D.: *Nature* **2020**, 581, 130
<https://doi.org/10.1039/D0CS01065K>
- [15] Wilkinson E., Giovanetti M., Tegally H. *et al.*: *Science* **2021**, 374(6566), 423.
<https://doi.org/10.1126/science.abj4336>
- [16] Zaher N.H., Mostafa M.I., Altaher A.Y.: *Acta Pharmaceutica* **2020**, 70(2), 145.
<https://doi.org/10.2478/acph-2020-0024>
- [17] Wang W., Xu Y., Gao R. *et al.*: *JAMA* **2020**, 323(18), 1843.
<https://doi.org/10.1001/jama.2020.3786>
- [18] Meshnick S.R.: *Med Trop (Mars)* **1998**, 58(3 Suppl), 13–7. PMID: 10212891
- [19] Chowdhury S., Mukherjee T., Mukhopadhyay R. *et al.*: *EMBO Molecular Medicine* **2012**, 4(10), 1126.
<https://doi.org/10.1002/emmm.201201316>
- [20] Jantan I., Haque M.A., Ilangkovan M., Arshad L.: *Frontiers in Pharmacology* **2019**, 10, 878.
<https://doi.org/10.3389/fphar.2019.00878>
- [21] Okoye N.N., Ajaghaku D.L., Okeke H.N. *et al.*: *Pharmaceutical Biology* **2014**, 52(11), 1478.
<https://doi.org/10.3109/13880209.2014.898078>
- [22] Riaz A., Rasul A., Hussain G. *et al.*: *Advances in Pharmacological and Pharmaceutical Sciences* **2018**, ID: 9794625.
<https://doi.org/10.1155/2018/9794625>
- [23] Patel J.I., Deshpande S.S.: *Anti-Inflammatory & Anti-Allergy Agents in Medical Chemistry* **2011**, 10(6), 442.
<https://doi.org/10.2174/1871523011109060442>
- [24] English B.J., Williams R.M.: *The Journal of Organic Chemistry* **2010**, 75(22), 7869.
<https://doi.org/10.1021/jo101775n>
- [25] Qian S., Fan W., Qian P. *et al.*: *Viruses* **2015**, 7(4), 1613.
<https://doi.org/10.3390/v7041613>
- [26] Mohan R., Hammers H., Bargagna-Mohan P. *et al.*: *Angiogenesis* **2004**, 7, 115.
<https://doi.org/10.1007/s10456-004-1026-3>
- [27] Mohammadi N.S., Özgüneş H., Başaran N.: *Turkish Journal of Pharmaceutical Sciences* **2017**, 14(2), 201.
<https://doi.org/10.4274/tjps.62207>
- [28] Gupta S.C., Patchva S., Aggarwal B.B.: *The AAPS Journal* **2013**, 15(1), 195.
<https://doi.org/10.1208/s12248-012-9432-8>
- [29] Chepanova A.A., Mozhaitsev E.S., Munkuev A.A. *et al.*: *Applied Sciences* **2019**, 9(13), 2767.
<https://doi.org/10.3390/app9132767>
- [30] Salehi B., Machin L., Monzote L. *et al.*: *ACS Omega* **2020**, 5(20), 11849.
<https://doi.org/10.1021/acsomega.0c01818>
- [31] Alagawany M., Abd El-Hack M.E., Farag M.R. *et al.*: *Animal Health Research Reviews* **2017**, 18(2), 167.
<https://doi.org/10.1017/S1466252317000081>
- [32] Baser K.H.C.: *Current Pharmaceutical Design* **2008**, 14(29), 3106.
<https://doi.org/10.2174/138161208786404227>
- [33] Sharma C., Al Kaabi J.M., Nurulain S.M. *et al.*: *Current Pharmaceutical Design* **2016**, 22(21), 3237.
<https://doi.org/10.2174/1381612822666160311115226>
- [34] Sen A.: *World Journal of Clinical Cases* **2020**, 8(10), 1767.
<https://doi.org/10.12998/wjcc.v8.i10.1767>
- [35] Alghasham A.A.: *International Journal of Health Sciences* **2013**, 7(1), 77.
<https://doi.org/10.12816/0006025>
- [36] Nahar L., Talukdar A.D., Nath D. *et al.*: *Molecules* **2020**, 25(21), 4983.
<https://doi.org/10.3390/molecules25214983>
- [37] Aditya S., Gupta S.: *Indian Dermatology Online Journal* **2013**, 4(3), 246.
<https://doi.org/10.4103/2229-5178.115538>
- [38] Lim S.H., Choi C.-I.: *Nutrients* **2019**, 11(2), 437.
<https://doi.org/10.3390/nu11020437>
- [39] Zhang H.-J., Rumschlag-Booms E., Guan Y.-F. *et al.*: *Journal of Natural Products* **2017**, 80(6), 1798.
<https://doi.org/10.1021/acsnatprod.7b00004>
- [40] Grosdidier A., Zoete V., Michielin O.: *Nucleic Acids Research* **2011**, 39, W270.

- <https://doi.org/10.1093/nar/gkr366>
- [41] Mengist H.M., Fan X., Jin T.: *Signal Transduction and Targeted Therapy* **2020**, 5(1), 67.
<https://doi.org/10.1038/s41392-020-0178-y>
- [42] Ferreira L.G., Dos Santos R.N., Oliva G., Andricopulo A.D.: *Molecules* **2015**, 20(7), 13384.
<https://doi.org/10.3390/molecules200713384>
- [43] Rahman M.M., Saha T., Islam K.J. et al.: *Journal of Biomolecular Structure and Dynamics* **2021**, 39(16), 6231.
<https://doi.org/10.1080/07391102.2020.1794974>
- [44] Jacobson M.P., Pincus D.L., Rapp C.S. et al.: *Proteins* **2004**, 55(2), 351.
<https://doi.org/10.1002/prot.10613>
- [45] Jacobson M.P., Friesner R.A., Xiang Z., Honig B.: *Journal of Molecular Biology* **2002**, 320(3), 597.
[https://doi.org/10.1016/S0022-2836\(02\)00470-9](https://doi.org/10.1016/S0022-2836(02)00470-9)
- [46] Morris G.M., Huey R., Lindstrom W. et al.: *Journal of Computational Chemistry* **2009**, 30(16), 2785.
<https://doi.org/10.1002/jcc.21256>
- [47] Jorgensen W.L., Tirado-Rives J.: *Proceedings of the National Academy of Sciences* **2005**, 102(19), 6665.
<https://doi.org/10.1073/pnas.0408037102>
- [48] Hall D.C. Jr., Ji H.-F.: *Travel Medicine and Infectious Disease* **2020**, 35, 101646.
<https://doi.org/10.1016/j.tmaid.2020.101646>
- [49] Guex N., Peitsch M.C.: *Electrophoresis* **1997**, 18(15), 2714.
<https://doi.org/10.1002/elps.1150181505>
- [50] Jin S.E., Ha H., Shin H.-K., Seo C.-S.: *Molecules* **2019**, 24(2), 265.
<https://doi.org/10.3390/molecules24020265>
- [51] Martini R., Esposito F., Corona A. et al.: *ChemBioChem* **2017**, 18(4), 374.
<https://doi.org/10.1002/cbic.201600592>
- [52] Vitor C.E., Figueiredo C.P., Hara D.B. et al.: *British Journal of Pharmacology* **2009**, 157(6), 1034.
<https://doi.org/10.1111/j.1476-5381.2009.00271.x>
- [53] Sultana T., Okla M.K., Ahmed M. et al.: *Molecules* **2021**, 26(24), 7696.
<https://doi.org/10.3390/molecules26247696>
- [54] Bugin K., Woodcock J.: *Nature Reviews Drug Discovery*, **2021**, 20, 254.
<https://doi.org/10.1021/acs.jnatprod.7b00004>
- [55] Liu J.: *Journal of Ethnopharmacology* **1995**, 49(2), 57.
[https://doi.org/10.1016/0378-8741\(95\)90032-2](https://doi.org/10.1016/0378-8741(95)90032-2)
- [56] Wang N., Liang H., Zen K.: *Frontiers in Immunology* **2014**, 5, ID: 614.
<https://doi.org/10.3389/fimmu.2014.00614>

Received 11 VI 2022